Transactions of the Japan Welding Society, Vol. 5, No. 2, September 1974

Effect of Sulphur on Solidification Cracking in Weld Metal of Steel (Report 4)*

—Theoretical and Experimental Iuvestigations on Solidification Crack Subceptibility of Low Carbon Steel Weld Metal—

By Hiroji NAKAGAWA**, Shunichi NISHINO**, Fukuhisa MATSUDA*** and Tomio SENDA**

Abstract

It is well known that manganese is an effective element to prevent the weld solidification crack in steel. Nevertheless not only the manganese content required for a given sulphur content but also the detailed metallurgical meaning on the effect of manganese have not been well understood so far. In this report these problems are theoretically discussed, by combining Fe-(Mn, Fe)S eutectic temperature in Fe-S-Mn phase diagram and the "changing curve in liquid composition" derived already by the authors. As the result, it is theoretically derived that a steel whose Mn^3/S is larger than 6.7 has a sufficiently low crack susceptibility. Then, this relation is experimentally confirmed for low carbon steels ($C \leq 0.12\%$) using the Trans-Varestraint test.

1. Introduction

Manganese is generally added to steel to prevent the detrimental effect of sulphur on the weld solidification crack. This is considered to be due to the formation of MnS of high melting temperature. Nevertheless the general relation between the manganese and sulphur contents necessary to sufficiently lower the solidification crack susceptibility and its metallurgical meaning are hardly revealed, since the studies have been mainly carried out only on the practical use so far.

On the other hand the authors in Report 2[1] theoretically derived the "changing curve in liquid composition" which gives the change in the composition of the remaining liquid during non-equilibrium solidification of Fe-S-Mn alloy steel, and predicted that the shape and the structure of sulphides and the solidification crack susceptibility can be classified by a new parameter Mn^3/S in the case where δ phase solidifies. This prediction was experimentally confirmed in Report 3[2] using the weld metals of Fe-S-Mn alloy steels. Further, by combining the "changing curve in liquid composition" and Fe-S-Mn phase diagram, the formation limit of FeS during the non-equilibrium solidification was predicted, and this was also experimentally confirmed[2].

In this report on the basis of these results, by further developing the combination of the "changing curve in liquid composition" and Fe-S-Mn phase diagram, the relation between the manganese and sulphur contents neccssary to minimize the solidification crack susceptibility is theoretically derived, and experimentally confirmed. For the experimental confirmation, low carbon steels are used, in which the carbon contents are not more than 0.12% and thus the effect of carbon on the solidification crack can be neglected. As regards the method of weld solidification crack test, the Trans-Varestraint test[3] is used.

2. Materials Used and Experimental Methods

2–1. *Materials Used*

The materials used for the solidification crack test were prepared by the following procedure. That is, a U-groove (4 mm depth × 10 mm width) was cutt off from the commercial plain carbon steel (JIS SS41 or SM41, 350 mm length × 150 mm width × 9 mm thickness) as shown in **Fig. 1.** This groove was filled with various amounts of powder of ferromanganese and ferrosulphur together with pure iron powder. A single pass of submerged-arc welding was laid on the filled groove with the welding current 500A (AC), arc voltage 30V and welding speed 200 mm/min. The flux and the wire used were Grade-80 and US-43 (4.8 mm diam.) respectively. The chemical com-

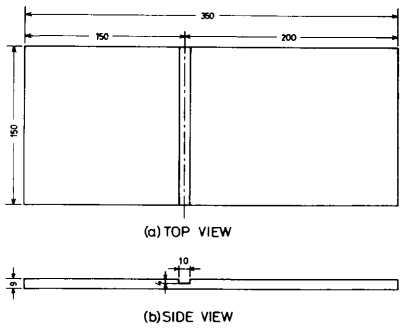

Fig. 1. Dimensions of the specimen for addition of manganese and sulphur using submerged-arc welding

* Received 17 May 1974

** H. Nakagawa is Instructor, S. Nishino is formerly Graduate Student and T. Senda is Professor of Welding Department, Faculty of Engineering, Osaka University, Suita, Osaka, Japan.

*** F. Matsuda is Associate Professor of Welding Reseaech Institute of Osaka University, Suita, Osaka, Japan.

Table 1. Chemical compositions of materials used for addition of manganese and sulphur using submerged-arc welding

MATERIAL	COMPOSITION (wt.%)				
	C	Si	Mn	P	S
SS 41	0.22	0.01	0.52	0.011	0.016
SM41	0.16	tr.	0.87	0.008	0.023
WIRE(US-43)	0.02	0.01	0.37	0.014	0.015

Table 2. Chemical compositions of weld metals obtained

MATERIAL	COMPOSITION (wt.%)				
	C	Si	Mn	P	S
SW-1	0.12	0.19	0.61	0.018	0.020
SW-2	0.11	0.16	0.91	0.019	0.017
SW-3	0.08	0.12	0.49	0.017	0.018
SW-4	0.10	0.05	0.32	0.016	0.019
SW-5	0.05	0.16	0.61	0.014	0.034
SW-6	0.10	0.18	1.08	0.020	0.035
SW-7	0.06	0.18	0.61	0.013	0.038
SW-8	0.08	0.22	0.68	0.018	0.038
SW-9	0.12	0.35	2.75	0.022	0.042
SW-10	0.12	0.23	1.41	0.019	0.045
SW-11	0.11	0.26	1.90	0.020	0.045
SW-12	0.07	—	0.56	—	0.045
SW-13	0.05	—	0.53	—	0.047
SW-14	0.03	—	0.59	—	0.052
SW-15	0.06	0.18	0.63	0.014	0.057
SW-16	0.05	0.16	0.51	0.013	0.070
SW-17	0.08	—	0.53	—	0.074
SW-18	0.04	0.12	0.48	0.015	0.081

positions of the base metal and the wire are shown in **Table 1.**

Then, after the stress relieving treatment at 650°C, 1 hr, the reinforcement of the submerged-arc weld bead was machined smooth to the surface. The chemical compositions of 18 different weld metals obtained are shown in **Table 2.** The carbon content was restricted to not more than 0.12%, since it is considered[4] that the detrimental effect of carbon on the solidification crack can be neglected if the content is less than 0.13%. It is also considered[4] that the detrimental effect of phosphorus can be neglected if the carbon content is less than 0.13%. As regards this, the authors also confirmed in a Trans-Varestraint test that the effect of phosphorus is far small in comparison with that of sulphur in the case of the carbon content not more than 0.12%[3]. Therefore these weld metals can be approximately regarded as Fe-S-Mn alloy steels from the viewpoint of the effects of sulphur and manganese on the solidification crack. Besides, in regard to the effect of oxygen, refer to Appendix I.

2–2. *Trans-Varestraint Test*

The specimen prepared as above mentioned was then set in the Trans-Varestraint apparatus as shown in **Photo. 1** so that the TIG-arc bead-on-plate weld

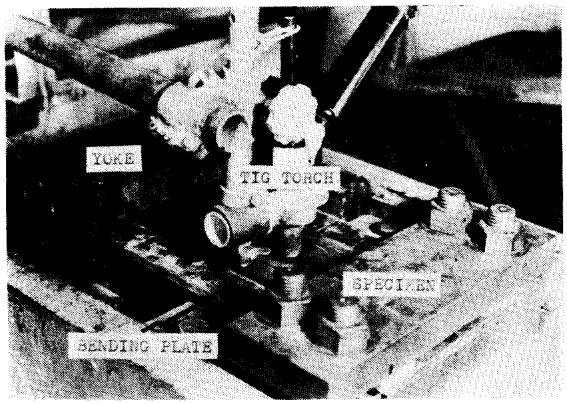

Photo. 1. Close-up view of Trans-Varestraint apparatus

in the test might be entirely confirmed to within the submerged-arc weld metal. In regard to the principle and the detail of the practical use of the Trans-Varestraint test, refer to reference 3. The TIG-arc bead-on-plate welding in the test was carried out with the conditions of welding current 250 A(DCSP), arc voltage 17～20 V and welding speed 150 mm/min.

There are some indices to evaluate the solidification crack susceptibility in the Trans-Varestraint test[3]. These are the cracking threshold, the maximum crack length, the number of cracks, the total crack length and the critical strain rate for temperature drop[3]. In this report the maximum crack length was adopted from among them, which is the length of the maximum crack generally formed at the weld center as shown in **Photo. 2.** The reason is that the maximum crack length can be correlated to the solidification brittleness temperature range (BTR)[3] which is the most important factor and that the BTR can be obtained from only one specimen as mentioned below:

Photo. 2. General appearance of the solidification cracks in Trans-Varestraint test

That is, the BTR is measured from a saturated value of the curve which shows the maximum crack length vs. augmented strain in the Trans-Varestraint test[3], and the maximum crack length reaches the saturated value at generally about 1% augmented strain[3]. Therefore the BTR can be obtained from the maximum crack length of only one specimen tested at 1% augmented strain. For these reasons the solidification crack susceptibility is evaluated in terms of the maximum crack length at 1% augmented strain.

2–3. *Thermal Analysis*

For Fe-S-Mn alloy steel the eutectic temperature of Fe-(Mn,Fe)S was measured by thermal analysis method in order to study the relation between it and the solidification crack susceptibility. **Table 3** shows the chemical compositions of the alloy steels, which were used in Report 3[2]. The sample was melted in an electric furnace of argon atmosphere, and the cooling curve was measured with a Pt/Pt+13%Rh thermocouple (0.5 mm diam.) and a self-balancing pen-writing recorder.

Moreover, for some of the alloys the melting phenomenon of the eutectic on a heating cycle was directly observed under a hot stage microscope in order to measure the melting-start temperature of the eutectic.

Table 3. Chemical compositions of materials used for thermal analysis

MATERIAL	COMPOSITION (wt.%)					
	C	Si	Mn	P	S	O
M- 4	0.007	0.07	1.00	0.008	0.072	0.012
M- 7	0.010	0.07	8.41	0.008	0.14	0.003
M- 9	0.007	0.07	3.80	0.008	0.24	0.003
M-10	0.006	0.01	0.39	0.008	0.28	0.010
M-12	0.006	0.01	1.16	0.008	0.31	0.021
M-14	0.006	0.01	0.53	0.008	0.38	0.010
M-15	0.006	0.01	0.64	0.008	0.42	0.013

3. Prediction as to Relation between Manganese and Sulphur Contents Necessary to Minimize Solidification Crack Susceptibility

The solidification crack is always formed at the primary grain boundary (including the cell or the cellular dendrite boundary) as shown in **Photo. 3.** Therefore the eutectic temperature of Fe-(Mn,Fe)S formed in the primary grain boundary should be investigated in order to clarify the effects of sulphur and manganese on the solidification crack.

Figs. 2(a) and **(b)** show Fe-S-Mn phase diagram[5] and its qualitative diagram. In Fig. 2(b) the curve e_3'E, which is Fe-(Mn,Fe)S binary eutectic curve, and the point R, which shows the maximum temperature (1510°C) on the eutectic curve e_3'E, are important in order to deal with the solidification process of the Fe-S-Mn alloy steels. For example, the composition of the remaining liquid of the alloy A_1 or A_2 in Fig. 2(b) during the solidification changes along the curve with an arrow drawn from the point A_1 or A_2. When this curve reaches the eutectic curve at the point b_1 or b_2, (Mn,Fe)S starts to solidify. Then, the remaining liquid composition of alloy A_1, whose curve has reached the point b_1 at the left side of the point R, moves toward the point E. On the contrary, the remaining liquid composition of the alloy A_2 moves toward the point e_3'. In regard to the detail of the solidification process, refer to Report 2[1].

The temperature 1510°C of the point R is slightly lower than the melting temperature of pure iron (1534°C). Therefore an alloy steel whose remaining liquid composition reaches the vicinity of the point R may have very low crack susceptibility, because the solidification temperature range is very narrow. Thus,

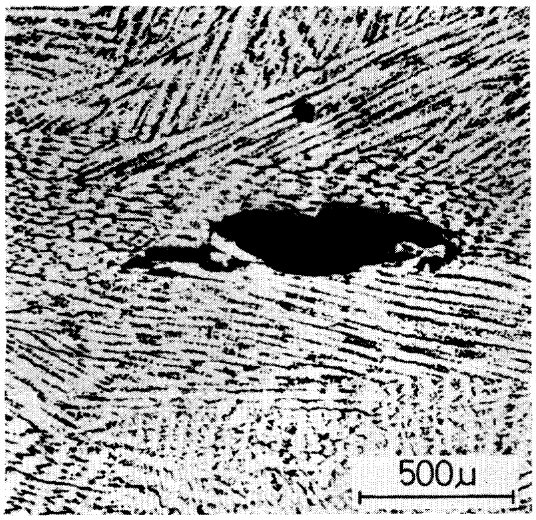

Photo. 3. An example of the relation between cracking location and solidification structure

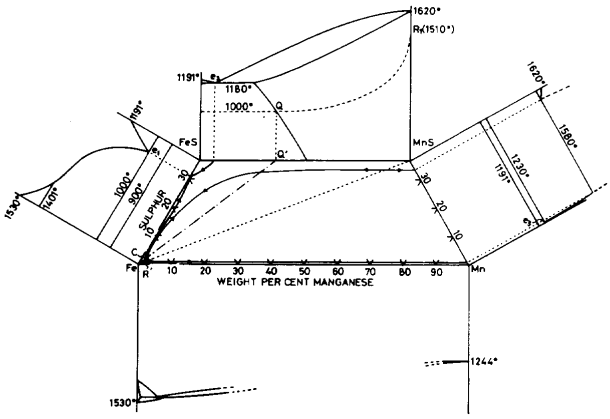

(a) actual diagram

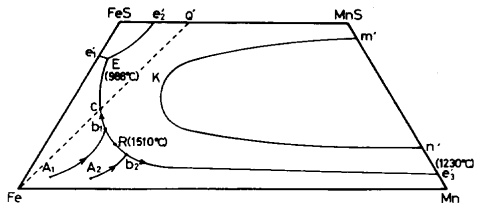

(b) qualitative diagram

Fig. 2. Fe-S-Mn phase diagram

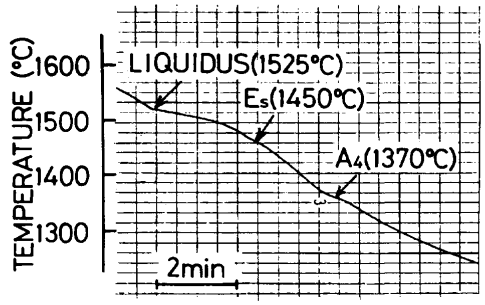

Fig. 3. An example of cooling curve of Fe-S-Mn alloy steel, sample: M-15

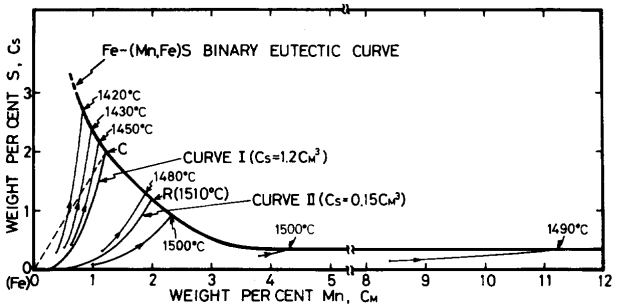

Fig. 4. Illustration of the eutectic temperature E_S in Table 4 on Fe-S-Mn phase diagram

in the following, this consideration is investigated in detail using the Fe-S-Mn phase diagram and the results of the thermal analysis, and then the relation between the manganese and sulphur contents necessary to minimize the solidification crack susceptibility is theoretically derived.

Fig. 3 shows, as an example, the cooling curve of alloy M-15 (0.64% Mn, 0.42% S) in Table 3. In this curve there are three crooked points at 1525°C, 1450°C and 1370°C. Among them the crooked point at 1525°C corresponds to the liquidus temperature. The crooked point at 1370°C is considered to be A_4 transformation temperature, judging from the little effect of sulphur on the transformation temperature, a little content of manganese and a slightly supercooled phenomenon on the cooling cycle. Therefore the crooked point E_S at 1450°C is considered to be the temperature at which the remaining liquid reaches the eutectic curve. **Table 4** shows the E_S point of each alloy steel obtained in the similar way.

Table 4. Temperature E_S at which Fe-(Mn, Fe)S eutectic starts to solidify

MATERIAL	E_S (°C)
M- 4	1500
M- 7	1490
M- 9	1500
M-10	1420
M-12	1480
M-14	1430
M-15	1450

On the other hand, the composition of the remaining liquid during the non-equilibrium solidification of Fe-S-Mn alloy steel changes along the "changing curve in liquid composition" on the Fe-S-Mn phase diagram, until the composition reaches the eutectic curve e_3'E[1]. The "changing curve in liquid composition" in the case where δ phase solidifies is given by[1]:

$$C_S^l = (C_S/C_M^3)C_M^{l\,3} \quad \cdots\cdots\cdots\cdots\cdots\cdots \quad (1)$$

where C_S^l and C_M^l: concentrations of sulphur and manganese in the remaining liquid respectively,

C_S and C_M: sulphur and manganese contents of the alloy.

Fig. 4 shows the eutectic temperature E_S in Table 4 on the Fe-S-Mn phase diagram, using Eq. (1). The point R in Fig. 4 is the maximum temperature point (1510°C) on the eutectic curve, and is well consistent with the distribution of the eutectic temperature. It is further observed that the eutectic temperature is lowered on both sides of the point R and that the lowering rate is larger on the left side than on the right side. In this connection, FeS together with (Mn,Fe)S was formed in the weld metals of the alloys M-10, 14 and 15 as already mentioned in Report 3[2], and these "changing curves in liquid composition" lie in the left region of CURVE I in Fig. 4. This means that the eutectics of these alloys do not finish the solidification until about 988°C which is Fe-(Mn,Fe)-FeS ternary eutectic point, though these start to solidify from 1420～1450°C as seen in Table 4 or Fig. 4.

Moreover, although FeS was not formed in the weld metal of M-12 as already mentioned in Report 3[2] whose "changing curve in liquid composition" reaches the eutectic curve at somewhat left side of the point R, the eutectic started to melt at 1100°C according to the direct observation under the hot stage microscope. **Photos. 4(a)** and **(b)** show the microstructures at pre-heating and at 1100°C respectively.

On the other hand, the eutectic of alloy M-9 started to melt at 1480°C, whose "changing curve in liquid composition" reaches the eutectic curve at 1500°C at the right side of the point R.

These facts suggest that the solidification crack susceptibility considerably differs according to whether the "changing curve in liquid composition" reaches the left side of the point R or the right side. That is to say, an alloy steel, for example the alloy A_1 in Fig. 2(b), whose "changing curve in liquid composition" reaches the left side may have a high crack susceptibility because of the wide solidification temperature range. On the contrary an alloy steel, for example the alloy A_2 in Fig. 2(b), whose "changing curve in liquid composition" reaches the right side may have a very low susceptibility because of the narrow solidification temperature range (about less than 50°C).

In order that the "changing curve in liquid composition" represented by Eq. (1) may reach the critical boundary point R, the sulphur content C_S must have the next relation with the manganese content C_M from Eq. (1):

$$C_S = 0.15C_M^3 \quad \cdots\cdots\cdots\cdots\cdots \quad (2)$$

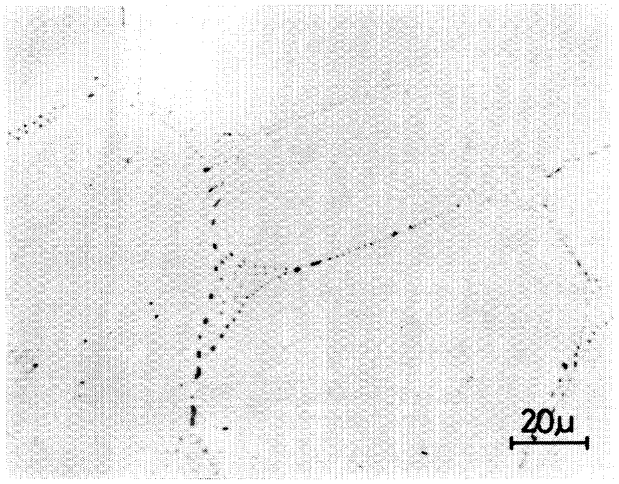

(a) at room temperature

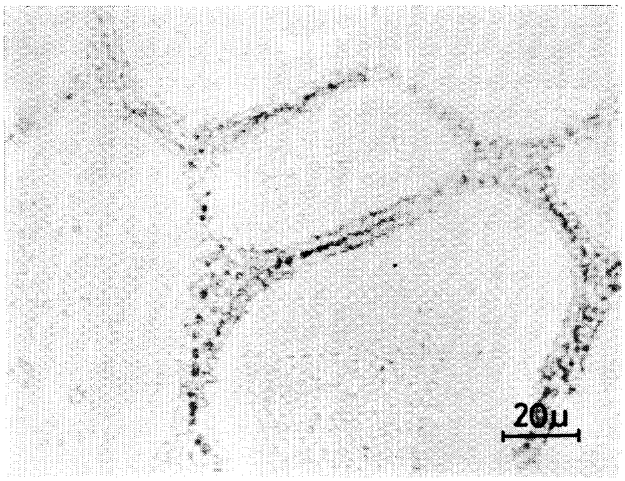

(b) at 1100°C

Photo. 4. Direct observation of eutectic melting on heating cycle under hot stage microscope, sample: M-12

Therefore, it is considered that the solidification crack susceptibility is sufficiently low for an alloy steel which satisfies the next relation:

$$C_S < 0.15 C_M^3 \quad \cdots\cdots\cdots\cdots\cdots\cdots \quad (3)$$

Using the parameter Mn^3/S[1], Eq. (3) can be represented as follows:

$$Mn^3/S > 6.7 \quad \cdots\cdots\cdots\cdots\cdots\cdots \quad (4)$$

Although the lower limit of the manganese content is given by Eq. (3) or (4), the upper limit must exist. According to the results in Table 4 or Fig. 4, however, the drop of the eutectic temperature at the right side is small even in the alloy M-7 containing about 8% manganese. Therefore there may be no necessity for paying attention to the upper limit in the commercial low carbon steel from the viewpoint of the solidification crack.

4. Experimental Confirmation of the Prediction

Fig. 5 shows the results of the Trans-Varestraint test on the materials in Table 2. The abscissa and the ordinate show the manganese and sulphur contents

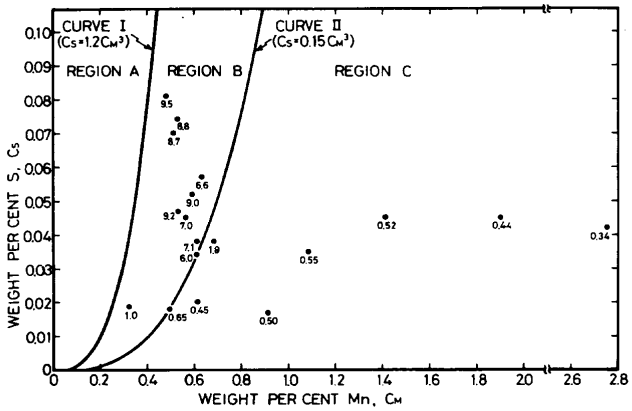

Fig. 5. Relation among manganese, sulphur contents and maximum crack length (in mm) obtained from Trans-Varestraint test

respectively, and the figure marking each experimental point represents the maximum crack length (in mm) at 1% augmented strain. Further, the CURVE I shows the formation limit of FeS in the non-equilibrium solidification as mentioned in Report 3[2], and the CURVE II shows Eq. (2) which gives the critical boundary for the solidification crack susceptibility.

According to the results, the maximum crack length has a small value (about 0.5 mm) in the right region of the CURVE II, and on the contrary that in the left region has a large value (about 6~9 mm). Examples of the appearance of solidification crack in each region are shown in **Photos. 5** and **6** respectively. Therefore Eq. (2) well agrees with the experimental results. Moreover the maximum crack length of

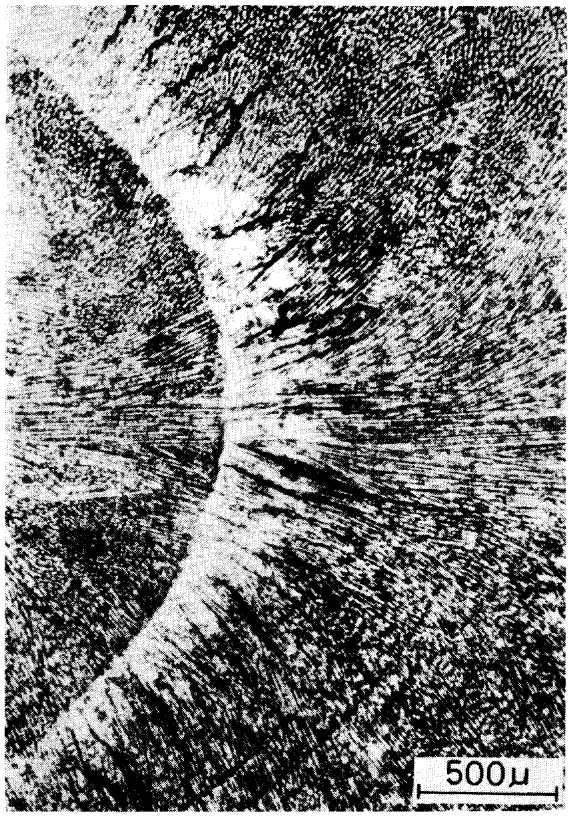

Photo. 5. An example of crack appearance in the right region of CURVE II, material: SW-6

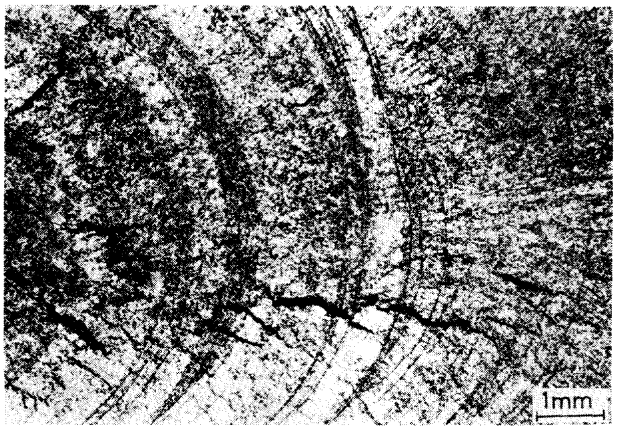

Photo. 6. An example of crack appearance in the left region of CURVE II, material: SW-15

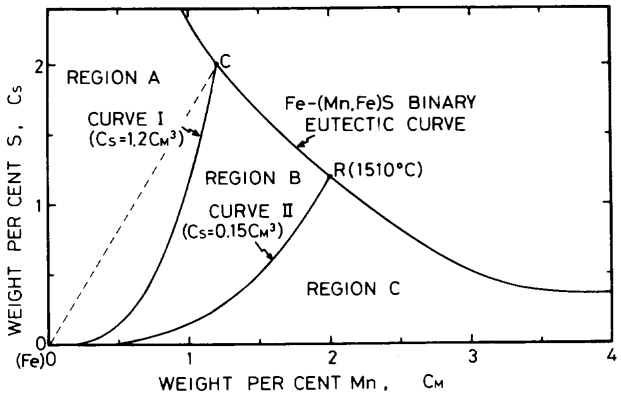

Fig. 8. Illustration of three regions which correspond to the changes in sulphide structure and solidification crack susceptibility

about 0.5 mm corresponds to the BTR of about 30～40°C, and this BTR value also well agrees with the solidification temperature range estimated from the eutectic temperature.

It was also verified that (Mn,Fe)S only is formed in the region between the CURVE I and II, by identifying the sulphides isolated electrolytically from the weld metals by X-ray diffraction technique (refer to Report 1[6] as regards the procedure). Therefore it is a necessary but not sufficient condition to lower the crack susceptibility that (Mn,Fe)S only be formed.

In order to further confirm the CURVE II, the results of the weld solidification crack susceptibility for carbon steels by Jones[7] was, then, investigated from the authors' viewpoint. **Fig. 6** shows the results by Jones, which were obtained by Murex type test. The abscissa and the ordinate represent the carbon content and Mn/S ratio, and the figure marking each experimental point represents the crack length in inches. The crack length of 2.5 inches means that the crack is formed over the whole length of weld bead. These results mean that the effect of carbon can be neglected in the case of the carbon content not more than 0.13%, though carbon has otherwise a detrimental effect. Thus the results for not more than 0.13% were rearranged in the same way as in Fig. 5. This is shown in **Fig. 7.** The crack length in Fig. 7 is also large in the left region of the CURVE II, and in the right region the crack is not formed at all with only one exception.

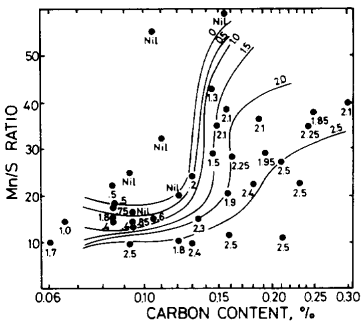

Fig. 6. Effect of carbon content and Mn/S ratio on severity of solidification cracking in Murex test on mild steel plstes[7]

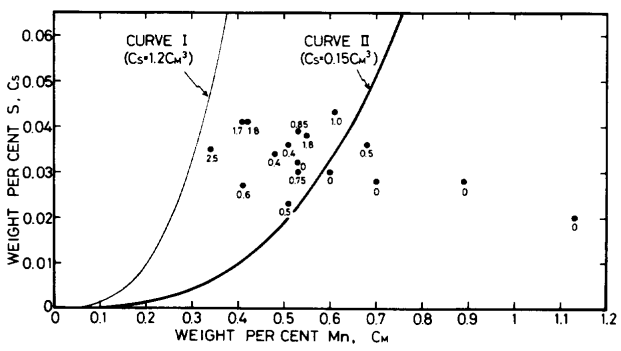

Fig. 7. Another representation of Fig. 6 (C≤0.13%)

Thus, according to the results obtained in this report and Report 3[2], the mutual effect of sulphur and manganese contents on the sulphides and on the solidification crack susceptibility can be classified into REGION A, B or C as shown in **Fig. 8.** In REGION A ($Mn^3/S<0.83$) FeS is formed together with (Mn,Fe)S, and therefore the solidification crack susceptibility is extremely high. In REGION B ($0.83<Mn^3/S<6.7$) (Mn,Fe)S only is generally formed, but the crack susceptibility is still high, since the eutectic temperature is low. In REGION C ($Mn^3/S>6.7$) the eutectic temperature of (Mn,Fe)S is high, and therefore the crack susceptibility is sufficiently low.

5. Conclusions

The relation between the manganese and sulphur contents necessary to minimize the weld solidification crack susceptibility was theoretically derived, and experi mentally confirmed for low carbon steel (less than 0.12% carbon) which could be approximated by Fe-S-Mn alloy steel. Main conclusions obtained are as follows:

(1) The solidification crack susceptibility can be lowered for a steel in which the remaining liquid composition changing during the weld solidification reaches the location of high eutectic temperature on Fe-S-Mn phase diagram. That is, the solidification crack susceptibility is sufficiently low in a steel whose manganese and sulphur contents satisfy the next relation:

$$Mn^3/S<6.7$$

This relation was experimentally confirmed by the Trans-Varestraint test and the Murex test.

(2) The mutual effect of manganese and sulphur contents on the sulphides and on the solidification crack susceptibility in the low carbon steel can be classified into REGION A, B or C on Fe-S-Mn phase diagram. In REGION A ($Mn^3/S<0.83$) FeS is formed together with (Mn,Fe)S, and therefore the solidification crack susceptibility is extremely high. In REGION B ($0.83<Mn^3/S<6.7$) (Mn,Fe)S only is generally formed, but the crack susceptibility is still high, since the eutectic temperature is low. In REGION C ($Mn^3/S>6.7$) the eutectic temperature of (Mn,Fe)S is high, and therefore the crack susceptibility is sufficiently low.

Acknowledgements

The authors would like to thank Mr. S. Hozumi of Katayama Iron Works Co. for his offering the materials, Mr. K. Watanabe and Mr. T. Matsuzaka of Hitachi Ltd. for their offering the Trans-Varestraint apparatus, and Mr. K. Kano of Kobe Steel Ltd. for his undertaking of chemical analysis.

Appendix I Effect of Oxygen on Solidification Crack

It is usually considered[8-11] that oxygen lowers the weld solidification crack susceptibility, because the increase in the oxygen content makes the shape of sulphide globular in the same way as the effect observed in the steel ingots[12-19]. In these reports[8-11] concerning the effect of oxygen on the solidification crack, however, the manganese and the sulphur contents lie in REGION A, B or near CURVE II in Fig. 8.

The authors also investigated the effect of oxygen using Fe-S-O ternary alloy steels, and the same result was obtained[20].

From these facts, it is understood that the crack susceptibility can be lowered to some extent by an increase in the oxygen content for a steel whose composition lies in REGION A or B. The increase in the oxygen content, however, may not be desirable, considering the detrimental effect of oxygen on the toughness of steel. Therefore it is advisable that manganese be added to REGION C instead of the increase in the oxygen content.

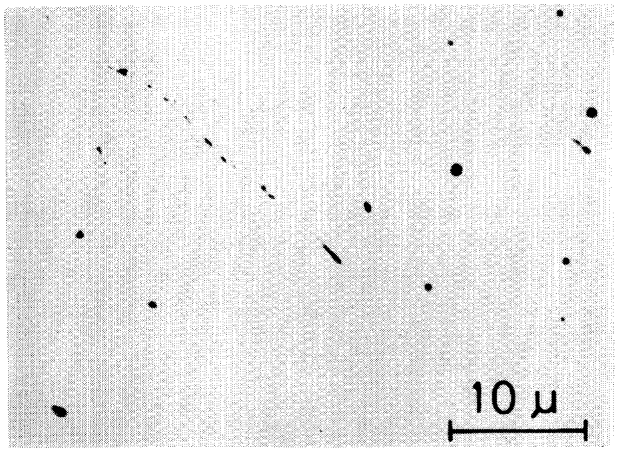

Photo. 7. Filmlike sulphides in weld metal of SW-15

In this report the oxygen content was about 0.03～0.04% in the steels tested with Trans-Varestraint test, because the materials were submerged-arc weld metals. **Photo. 7** shows, as an example, the microstructure of the tested weld metal of SW-15 in Table 2, which lies in REGION B, and a filmlike sulphide ((Mn,Fe)S) is observed. Therefore it is considered that the oxygen content hardly affects the results in this report.

Appendix II Evaluation of Solidification Crack Susceptibility

The solid curve in **Fig. 9** qualitatively shows the ductility of a material during the weld solidification. This curve can be obtained with the Trans-Varestraint test[3]. The temperature range surrounded by the ductility curve is the brittleness temperature range (BTR), which was the index used to evaluate the crack susceptibility in this report. Considering, however, that the increase in the actual strain applied in the fabricating weldments may be approximated by the broken line a, b or c as shown in Fig. 9, the inclination of the tangential broken line b to the ductility curve should be the most reasonable index[3]. This inclination is called the critical strain rate for temperature drop (CST)[3]. Refer to reference 3 as regards the detail.

The relation between the BTR and the CST was, then, investigated. The materials used are some

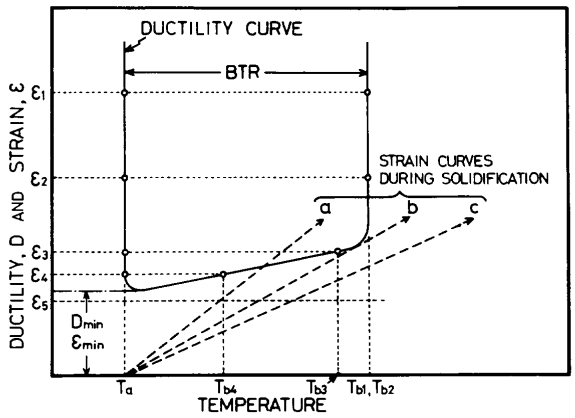

Fig. 9. Schematic representation of ductility curve, solidification brittleness temperature range (BTR) and strain curve

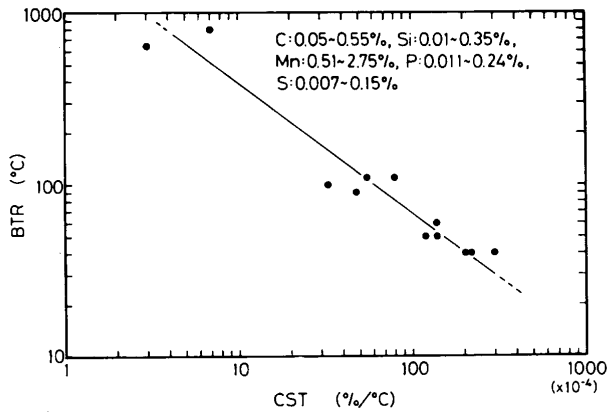

Fig. 10. Relation between BTR and CST in weld metal of steel

items in Table 2 and the commercial structural steels used in reference 3 and so on. **Fig. 10** shows the result, and it is observed that log BTR is nearly in a linear relation with log CST. Therefore it is considered that the measurement of only the BTR is sufficient to evaluate the crack susceptibility in the steel.

References

1) H. Nakagawa, F. Matsuda and T. Senda: Trans. JWS, Vol. 5 (1974), No. 2, pp.
2) H. Nakagawa, F. Matsuda, T. Senda, T. Matsuzaka and K. Watanabe: Trans. JWS, Vol. 5 (1974), No. 2, pp.
3) T. Senda, F. Matsuda, G. Takano, K. Watanabe, T. Kobayashi and T. Matsuzaka: Trans. JWS, Vol. 2 (1972), No. 2, pp. 45–66.
4) J.C. Borland: British Weld. J., Vol. 8 (1961), pp. 526–540.
5) R. Vogel und W. Hotop: Arch. Eisenhütt., 11 (1937/38), 41–54.
6) H. Nakagawa, F. Matsuda and T. Senda: Trans. JWS, Vol. 5 (1974), No. 1, pp. 39–46.
7) P.W. Jones: British Weld. J., Vol. 6 (1959), pp. 282–290.
8) T. Boniszewskii, S.E. Dieu and H.F. Tremlett: British Weld. J., Vol. 13 (1966), pp. 558–577.
9) T. Boniszewski and S.E. Dieu: British Weld. J., Vol. 14 (1967), pp. 132–144.
10) V.V. Podgaetskii, G.I. Parfessa and S.M. Litvinchuk: Avt. Svarka, 1969, No. 3, pp. 19–23.
11) E.J. Morgan-Warren and M.F. Jordan: J. Iron Steel Inst., Vol. 210 (1972), pp. 868–879.
12) AIME: "Basic Open Hearth Steelmaking", Third Edition, 1964.
13) C.E. Sims: Trans. Met. Soc. AIME, Vol. 215 (1959), pp. 367–393.
14) R. Kiessling, S. Bergh and N. Lange: J. Iron Steel Inst., Vol. 201 (1963), pp. 965–967.
15) W. Dahl, D. Hengstenberg und C. Düren: Stahl u. Eisen, 86 (1966), 782–795.
16) R.B.G. Yeo: J. Metals, Vol. 19 (1967), No. 6, pp. 29–32.
17) R.B.G. Yeo: J. Metals, Vol. 19 (1967), No. 7, pp. 23–27.
18) S. Marich and R. Player: Met. Trans., Vol. 1 (1970), pp. 1853–1857.
19) P.P. Mohla and J. Beech: Brit. Foundryman, Vol. 61 (1968), pp. 453–460.
20) T. Senda, F. Matsuda, H. Nakagawa, T. Iwasaki, K. Watanabe and T. Matsuzaka: J. Japan Weld. Soc., Vol. 42 (1973), pp. 1073–1084 (in Japanese).